Vol. 69: 193–207, 2016
doi: 10.3354/cr01405

CLIMATE RESEARCH
Clim Res

Published online August 17

High precipitation and low evaporation resulted in high lake levels of the Juyanze paleolake, northwest China, during 34–26 cal kyr BP

Zhuolun Li*, Nai'ang Wang, Xunhe Zhang, Hongyi Cheng, Yu Li

College of Earth and Environmental Sciences, Center for Desert and Arid Region Research, Lanzhou University, Lanzhou 730000, PR China

ABSTRACT: This study addressed the lake evolution of the Juyanze paleolake with the goal of calculating precipitation and evaporation during 34–26 cal kyr BP, which will aid evaluation of the reliability of using lake level changes to assess past changes in climate. Fourteen paleoshorelines were recognized at the Juyanze paleolake, and ^{14}C dating results showed that the highest 8 formed during 34–26 cal kyr BP. A unified Juyanze paleolake with an area of 7601 km^2 reached 932 m above sea level (a.s.l.) at 34 cal kyr BP. The paleolake then decreased to an area of 6104 km^2 and an elevation of 930 m a.s.l. at 32 cal kyr BP, and to 5589 km^2 and 926 m a.s.l. at 26 cal kyr BP. Using water and energy balance equations, catchment paleo-precipitation and paleo-runoff were calculated for 3 previous periods. The results revealed that the catchment of the Heihe River required approximately 177 ± 29 mm yr^{-1} of precipitation to sustain the maximum lake area, which is a 32% increase compared with the modern value. Runoff from rivers to the lake was 61.9 × 10^8 m^3 at 34 cal kyr BP, with a calculation error of ±22.3 × 10^8 to 29.7 × 10^8 m^3. The humid climate and high lake levels of Juyanze paleolake that occurred during 34–26 cal kyr BP might have resulted from an enhanced monsoon. Moreover, low levels of evaporation may also have affected moisture changes.

KEY WORDS: Climate change · Lake evolution · Late Quaternary · Paleolake · Arid region

Resale or republication not permitted without written consent of the publisher

1. INTRODUCTION

The evolutionary history of paleolakes has been used to reconstruct late Quaternary (last 100 kyr BP) environmental and climatic conditions in the deserts to the northeast of the Tibetan Plateau (Pachur et al. 1995, Zhang et al. 2002a, Wang et al. 2011, Long et al. 2012). However, the paleolake evolution and the hydrological cycle of the late Quaternary in this area are very complex (Lehmkuhl & Haselein 2000). Climate change in the region is influenced by the combined effects of the Asian summer monsoon and westerly winds (Yang et al. 2011, Li et al. 2012a), and changes in these 2 climate systems could have produced changes in the lake levels and the hydrological cycle in this area during the late Quaternary (Zhao et al. 2007, Yu & Shen 2010, Long et al. 2012). For some terminal lakes of inland rivers, glacial meltwater is also a key factor that could have driven changes in lake levels (Yang et al. 2002, Jiang et al. 2011, Yan & Zheng 2015). Moreover, non-climatic factors, such as neotectonics, also affected lake evolution during the late Quaternary (Hartmann & Wünnemann 2009). Hence, the mechanism of late Quaternary lake evolution in this area remains unclear. Understanding this mechanism will aid evaluation of the reliability of using lake level changes to assess past environmental changes.

The Juyanze paleolake, located in the Ejina (Gaxun Nur) Basin to the north of the Tibetan Plateau, was a

*Corresponding author: lizhuolunlzl@163.com

© Inter-Research 2016 · www.int-res.com

terminal lake at the northwest margin of the Badain Jaran Desert. Previously reported preliminary investigations have shown that high lake levels were present during 40–25 cal kyr BP at the Juyanze paleolake and also in the nearby Badain Jaran Desert and Tengger Desert (Pachur et al. 1995, Zhang et al. 2004, Wang et al. 2011, Yang et al. 2011). The results of these investigations revealed that paleolake evolution was affected by climate change and indicated that the climate during the previous periods was different from that of the present in areas of NW China that are now arid to hyperarid. Some studies have synthesized paleoclimate records and discussed the possible causes of the paleoclimate change. Shi et al. (2001) suggested that an enhanced Indian Monsoon caused higher precipitation during 40–30 cal kyr BP. However, Yang et al. (2004) hypothesized that intensified westerly circulation was responsible for increased moisture over NW China and may have caused a humid environment. Yang & Scuderi (2010) argued that an enhanced Indian Monsoon is insufficient to explain the extensive lakes that occurred in the deserts of China during the Pleistocene. Hence, the evolution of these paleolakes under the effects of climate change is still under discussion. Moreover, strong, recent tectonic activities in the area have had a large impact on lake formation in the basin during the Holocene (Zhang et al. 2006, 2013, Hartmann & Wünnemann 2009). However, whether such tectonic activities affected the evolution of paleolakes in the region remains unclear. Therefore, the formation mechanism of the Juyanze paleolake and the lake's evolutionary history during 40–25 cal kyr BP also remain uncertain.

An approach to reconstructing the lake surface areas and past hydrology of the lake basins is to investigate constructional, sandy lake shoreline features (Long et al. 2012, Huth et al. 2015). Shoreline deposits do not provide continuous high-resolution climate records, but they do provide a quantitative record of large hydrologic changes to the lake system through the relationship between the basin water budget and the exact surface areas of the paleolake system at shoreline levels of known age. Water and energy balance equations have been applied to reconstructions of past hydrologic changes in drainage basins (Kutzbach 1980, Hastenrath & Kutzbach 1983, 1985, Bergonzini et al. 1997, Hoelzmann et al. 2000, Jia et al. 2001, Rhode et al. 2010, Huth et al. 2015). Therefore, shoreline deposits are an ideal method for quantifying past hydrologic changes of paleolakes down to millennial timescales.

To address previously unanswered questions, we here present a study on the evolution of the Juyanze paleolake with the goal of calculating precipitation and evaporation during 34–26 cal kyr BP. We employed ^{14}C dating of the paleoshorelines to reconstruct the lake surface areas and then used water and energy balance equations to calculate evaporation, catchment precipitation, and runoff from rivers to the lake. We also discuss the evolution mechanism of the Juyanze paleolake during 34–26 cal kyr BP.

2. STUDY SITE

The Juyanze paleolake is a terminal lake at the northwest margin of the Badain Jaran Desert, which is located in the Ejina (Gaxun Nur) Basin to the north of the Tibetan Plateau. The Ejina Basin, covering an area of approximately 28 000 km^2, is one of the largest inland basins in arid NW China (Fig. 1). The basin is filled with 300 m thick Quaternary lacustrine sediments, such as clay and silt, locally interrupted by fluvial and eolian sand (Hartmann & Wünnemann 2009). The lowest elevation of the sill in the basin exceeds 940 m. Geologically, it is within part of the Alashan Plateau and is located in western Inner Mongolia (40° 30′ to 43° 30′ N, 99° 45′ to 101° 45′ E) (Zhang et al. 2006). The basin is an intramontane accumulation area between the Qilian Mountains to the south and the Gobi-Tianshan Mountains to the north. Both of these mountain ranges are influenced by left-lateral plate motions accompanied by intense vertical displacements due to the ongoing collision of the Indian plate with the Eurasian continent. Consequently, the Ejina Basin has developed as a large pull-apart basin between these structural elements, acting as a base for the Heihe River drainage system from the NE Tibetan Plateau (Zhang et al. 2006, Becken et al. 2007).

Three terminal paleolakes (the Gaxun Nur, Sogo Nur, and Juyanze) were distributed within the Ejina (Gaxun Nur) Basin (Fig. 1). The terminal lakes had an area of more than 7000 km^2 during 40–30 cal kyr BP (Wang et al. 2011). However, Juyanze Lake has shrunk to the small Jinsutu Lake (also called Swan Lake) in the NE corner of the basin (Fig. 1). Sogo Nur, also called Eastern Juyan Lake, is currently an artificial lake, with an area of approximately 30 km^2 in 2003. Very shallow (<1 m) and rather small water bodies, which are fed by groundwater and sporadic runoff from branches of the Heihe River, currently exist within the basin (Mischke et al. 2003). The Heihe River drains a large area including the Qilian Mountains in the south. The highest ice-covered peaks within the catchment area exceed an elevation of 5500 m.

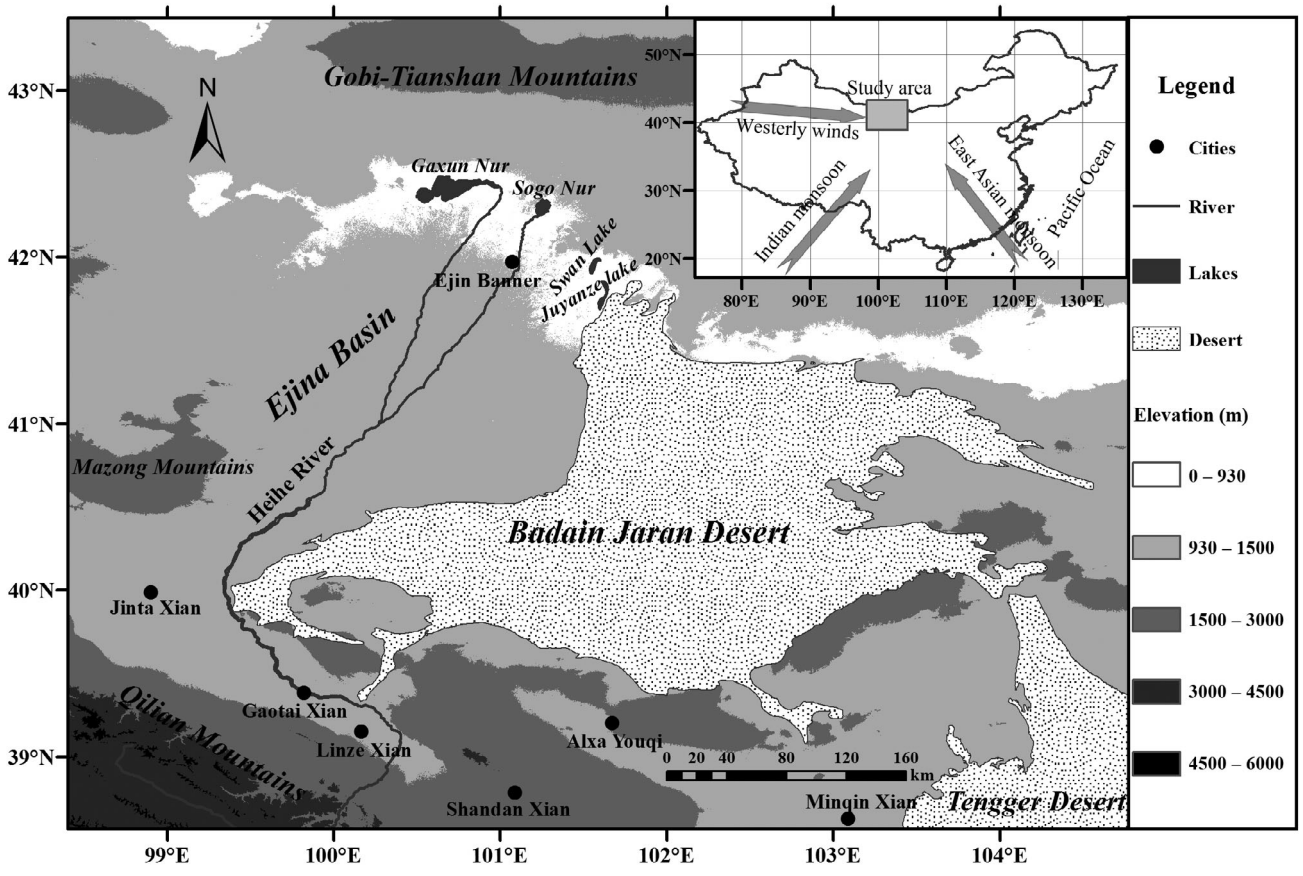

Fig. 1. Location of the study area

The basin is subject to a climate with strong seasonal contrasts (Mischke et al. 2003), and the present-day climate is extremely dry and continental. According to meteorological data, the average annual precipitation in Ejin Banner (41° 57′ N, 101° 04′ E; 940.5 m above sea level [a.s.l.]) is 35.5 mm (Ma et al. 2011), whereas the mean annual evaporation rate from water surfaces is approximately 2345 mm yr^{-1} (Shen et al. 2013). The rainfall in the basin is derived from the Asian summer monsoons at present (Conroy & Overpeck 2011). Moreover, more than half of the precipitation falls in June to August, and July is normally the month with the highest rainfall. According to the seasonal distribution of evaporation in this area, the ratio of the evaporation in winter to the total annual evaporation is only 5 to 7%. The lake is iced over for <2 mo in winter. The annual mean temperature is 8°C, and the January and July means are −12.5 and 26.2°C, respectively (Zhang et al. 2006). However, in the upper catchment of the Heihe River, the annual mean temperature decreases to −3 to 3°C, and the annual precipitation is approximately 350 to 400 mm, most of which occurs during summer (Ding et al. 2009). The average annual precipitation of the entire catchment is about 134 mm.

3. MATERIALS AND METHODS

3.1. Paleolake level indicators and ages

Paleoshorelines, which formed when sufficient wave and wind energy existed to build constructional landforms that persisted in the landscape, are unequivocal evidence of lake highstands (Rex 1961, Gracia Prieto 1995, Lazarus & Murray 2011). In the arid region of NW China, sandy lake shorelines formed at times when the lake surface was relatively stable while in retreat. These resulted in the formation of a series of shorelines in the shape of concentric circles or parallel lines (Wang et al. 2011). Therefore, the areas and levels of the paleolake can be reconstructed from the paleoshorelines.

During the field investigations, the GPS coordinates of all the paleoshorelines were measured on-site using a high-precision GPS unit. The elevations of the paleoshorelines and areas of the paleolake were then plotted onto 1:50 000 scale topographic maps.

Shells were collected from the paleoshoreline layers. To avoid inconsistencies, we chose mollusk shells of the same species (*Radix auriculata*) that did not appear to have been reworked, indicating that the shell samples had not been transported after deposition. The shells used for dating were analyzed by X-ray diffraction to ensure that they consisted only of aragonite without any recrystallization, in order to be certain that carbonate exchange between the groundwater and the shells had not occurred. All of the samples were processed using HNO_3 to remove any trace of organic components and were then dated by accelerator mass spectrometry (AMS) ^{14}C dating at the Laboratory of Scientific Archaeology and Preservation of Cultural Relics, School of Archaeology and Museology, Peking University, China.

Incorporation of ^{14}C-deficient (or 'dead') carbon from limestone and other carbonate rocks may cause some dating results to be older than their true age, which is the principle of the reservoir effect. Hartmann & Wünnemann (2009) reported that the reservoir effect may increase the apparent age of sediment samples from this area to the possible extent of a few hundred years. However, Zhang et al. (2006) suggested that there had been strong reworking of the sediments in the Ejina Basin during and after deposition. In fact, this reworking effect, which would lead to older sediments being transported and deposited in the younger layer, could significantly complicate ^{14}C dating of the lake sediments in the arid region of NW China, possibly to a greater extent than the reservoir effect (Li et al. 2012b). Therefore, the reservoir effect on sediment samples from the Juyanze paleolake is uncertain, and a possible error of a few hundred years could be caused by the reworking effect and not by the reservoir effect. Moreover, it is still unclear whether the mollusks (*R. auriculata*) consistently incorporate dead carbon from limestone into their shells when it is available (Pigati et al. 2010). In this study, we focused on the ^{14}C ages of the mollusk shell samples at the millennial time scale. Although the dating results may be somewhat older than their true age, this difference should not influence the results at the millennial time scale. Thus, the ^{14}C dating results used in this study were not corrected for a reservoir effect.

The radiocarbon dates were converted to calendar years using the Calib 7.0 radiocarbon calibration program, which is based on the IntCal 13 Radiocarbon Calibration Data Set described by Reimer et al. (2013).

3.2. Evaporation calculation

Water surface and land surface evaporation can be acquired by the energy balance formula (Kutzbach 1980):

$$E = \frac{R'}{(1+B)L} \quad (1)$$

where R' is the net radiation (W m^{-2}), B is the Bowen ratio, and L is the latent heat of vaporization (2.5×10^6 J kg^{-1}). Net radiation can be calculated using the following formula:

$$R' = KG(1-\alpha)(1-C) - A\varepsilon\delta T^4 \quad (2)$$

where K is the atmospheric transmission coefficient, G is the insolation at the top of the atmosphere (W m^{-2}), α is the surface reflectivity, C is the cloud-sky cover ratio (in tenths), A is the Ångström coefficient, ε is the surface emissivity, δ is the Stefan-Boltzmann constant (5.67×10^{-8} $\frac{W}{m^2 K^4}$), and T is the air temperature (K). The formula for calculating the Ångström coefficient is:

$$A = (a_1 - b_1\sqrt{e}(1 - c'C^2) \quad (3)$$

where c' is the Berliand latitude coefficient, e is the water vapor pressure (mb), C is the cloud-sky cover ratio (in tenths), and a_1 and b_1 are coefficients that are used to correct the value of the net long-wave radiation under cloudless skies (Berliand 1952).

Eqs. (1) to (3) show that the net shortwave radiation, net longwave radiation, and Bowen ratio significantly affect evaporation. In addition, the Ångström coefficient must be corrected, and different values can cause large variability in the calculated results (Li et al. 2013). Li et al. (2013) corrected the Ångström coefficient using modern meteorological data for the lower reaches of the Heihe River, and the resulting equations allow highly accurate calculations of evaporation. As Table 1 shows, the differences between the calculated and measured net longwave radiation and evaporation values are within 2% (Li et al. 2013). Therefore, the Ångström coefficient was calculated using Eq. (3). On the land surface, a_1 and b_1 were defined as 0.39 and 0.058, respectively (Berliand 1952), and as 0.535 and 0.07, respectively, on the water surface, as suggested by Li et al. (2013).

Table 1. Calibrated water and energy balance values (1993 to 2009). Source: Li et al. (2013)

	Observed	Simulated	Error (%)
Net long-wave radiation (W m^{-2})	121.52	120.05	−1.2
Evaporation (mm)	2345	2378	−1.4
Runoff (10^8 m^3)	9.26	8.57	−7.5

3.3. Hydrologic budget modeling

To quantify the hydrologic record, we employed catchment precipitation and runoff models to estimate the climatic conditions required to sustain the lake system at the higher lake levels in the past.

In closed-basin lake systems, the basin-averaged seepage is regarded to be zero. The basic hydrologic mass balance model for a closed-basin lake must balance input from precipitation to the catchment (both land and lake) with output through evaporation from the catchment in order to maintain the lake level at a steady state and thus form a shoreline (Kutzbach 1980, Bergonzini et al. 1997, Hoelzmann et al. 2000, Jia et al. 2001, Rhode et al. 2010):

$$PS = E_u S_u + E_m S_m + E_l S_l \quad (4)$$

where P and S represent catchment precipitation and catchment area, E_u, E_m, and E_l represent evaporation in the upper, middle, and lower reaches of the catchment, and S_u, S_m, and S_l represent the area of the upper, middle, and lower reaches of the catchment, respectively. The values of S for each reconstructed lake level of known age were calculated using 1:50 000 scale topographic maps. The values of E_u, E_m, and E_l were calculated using Eqs. (1) to (3).

The Juyanze paleolake was a closed-basin lake system during the late Quaternary (Wang et al. 2011). When the lake level was at a steady state and a shoreline was thus formed, input from direct precipitation on the lake and runoff from rivers to the lake must have been balanced with output through evaporation from the lake (Li et al. 2013):

$$P_w S_w + R = E_w S_w \quad (5)$$

where P_w represents the precipitation at the water surface, which can be inferred from paleo proxy records, S_w represents the water surface area, R is the runoff from rivers to the lake, and E_w is the evaporation at the water surface, which can be calculated using Eqs. (1) to (3). Therefore, the runoff from rivers can be calculated using Eqs. (1) to (3) and (5). To clarify whether these equations could calculate the runoff from rivers in this area, Li et al. (2013) selected meteorological data and hydrological data, and reconstructed the annual average runoff from rivers in this area during 1993 to 2009. Their results indicated that the difference between the calculated and measured runoff values from rivers was only 7.5% (Li et al. 2013).

4. RESULTS

4.1. Evolution of the Juyanze paleolake during 34–26 cal kyr BP

During our field investigations, 14 paleoshorelines, some of which can be seen in the satellite image (Fig. 2a), were recognized in the eastern portion of Jinsutu Lake (Swan Lake) (Fig. 2a,b). The exact elevations of the shorelines are presented in Table 2. The highest paleoshorelines (B1), consisting of 4 to 5 small paleoshorelines, are 932 m a.s.l. with a width of approximately 30 m (Fig. 2c,d). The sediments consisted of small gravel, sand, and silt. The other paleoshorelines are lower than 930 m a.s.l. (Table 2). Moreover, in the northern part of Jinsutu Lake (Swan Lake), a paleoshoreline occurs at 926 m a.s.l., which is the same elevation as that of the eighth shoreline (B8) (Fig. 2a,e).

Mollusk (*Radix auriculata*) shells only occurred in layers of the 3 paleoshorelines (B1, B2, and B8) with depths of 0 to 30 cm. They were collected from the sites of B1 (42° 0′ 13″ N, 101° 40′ 19″ E), B2 (41° 59′ 03″ N, 101° 40′ 22″ E), and B8 (42° 01′ 15″ N, 101° 33′ 22″ E) (Fig. 2a,c,e). The AMS ^{14}C dating results, including some ^{14}C dating results reported previously by Pachur et al. (1995), are presented in Table 3. This table shows that none of the dates from the paleoshorelines are inversional. Moreover, the similar ^{14}C ages of mollusk shells and carbonate (34.15 and 33.89 cal kyr BP, respectively) in the highest paleoshorelines (B1) also suggest that the dates listed in Table 3 are reasonable, indicating that B1 formed at 34 cal kyr BP. The ^{14}C ages of mollusk shells showed that B2 formed at 31.536 (31.159 to 31.913) cal kyr BP. Although this dating result may be somewhat older than its true age, the difference should not influence the results at the millennial time scale. Thus, the formation of B2 at 32 cal kyr BP can be accepted. Additionally, mollusk shells collected from B8 were dated to 25.58 cal kyr BP, and carbonate from B9 was dated to 20.83 cal kyr BP (Pachur et al. 1995). Therefore, it can be inferred that the paleoshorelines (B1 to

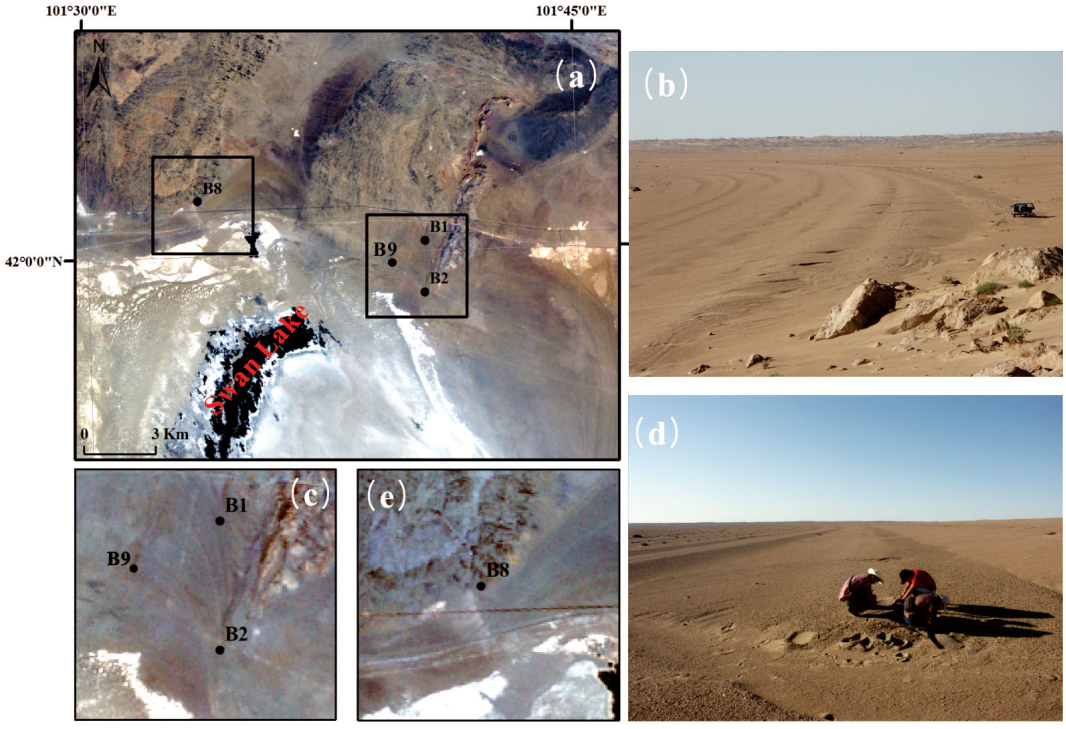

Fig. 2. The Juyanze paleolake. (a) Satellite image of lake shorelines. (b) Close up of lake shorelines. (c) Satellite image of lake shorelines B1, B2, and B9. (d) First shoreline (B1; 932 m). (e) Satellite image of shoreline B8 (926 m)

B8) are vestigial evidence of the high lake levels during 34–26 cal kyr BP.

The reconstructions of the areas and extents of the Juyanze paleolake during the periods mentioned above indicate that a unified Juyanze paleolake with an area of 7601 km^2 occurred at 34 cal kyr BP (Fig. 3). The paleolake then decreased to 6104 km^2 at 32 cal kyr BP and to 5589 km^2 at 26 cal kyr BP (Fig. 3).

Table 2. Altitudes of the paleoshorelines at the Juyanze paleolake

Paleo-shorelines	Latitude (N)	Longitude (E)	Altitude (m)
B1	42° 0′ 14″	101° 40′ 23″	932
B2	42° 0′ 13″	101° 40′ 17″	929.9
B3	42° 0′ 13″	101° 40′ 15″	929.5
B4	42° 0′ 14″	101° 40′ 15″	929.1
B5	42° 0′ 13″	101° 40′ 14″	928.8
B6	42° 0′ 13″	101° 40′ 13″	928.5
B7	42° 0′ 12″	101° 40′ 12″	928.1
B8	42° 0′ 12″	101° 40′ 8″	926
B9	42° 0′ 10″	101° 39′ 58″	923
B10	42° 0′ 9″	101° 39′ 57″	922.5
B11	42° 0′ 58″	101° 32′ 52″	918.2
B12	42° 0′ 55″	101° 32′ 55″	916.7
B13	42° 0′ 41″	101° 32′ 59″	911.7
B14	42° 0′ 40″	101° 33′ 0″	910.5

4.2. Paleo-environment parameters during 34–26 cal kyr BP

The paleo-environment parameters were calculated using the following steps:

G was calculated by Berger (1978), as presented in Table 4. K varies with latitude and is considered to be 0.76 to 0.78 from 30° to 45° N (Xu 1994). In this study, K was assumed to be 0.77, based on the range of the study area (Table 4).

Parameters C and e were calculated on the basis of the results of Jia et al. (2000, 2001, 2004), using modern meteorological data measured in another area. The area selected for the present period must have the same radiation, same underlying surface, and similar altitude as the study area during the reconstruction periods (Jia et al. 2000, 2001, 2004). The selected locations were modified slightly to match the variations in radiation during the reconstruction periods. Therefore, modern meteorological data from the Tibet Plateau was used to calculate C and e for the upper reaches, and data from arid regions was used for the middle and lower reaches. The relevant results for C and e are presented in Table 4.

The water surface reflectivity (α) was defined as 0.08, based on observations of the annual mean reflectivity at a latitude of 40° N (Budyko & Miller

Table 3. ^{14}C ages of high lake levels of the Juyanze paleolake

Sample No.	Coordinates Latitude (N)	Longitude (E)	Altitude (m)	Dating material	^{14}C data (kyr BP)	cal kyr BP (2σ)	References
B1	42° 0′13″	101° 40′19″	932	Mollusk shells	29.480 ± 0.095	34.15 (33.667–34.663)	This study
			932	Carbonate	29.4 ± 0.45	33.89 (32.922–34.850)	Pachur et al. (1995)
B2	41° 59′03″	101° 40′22″	929.9	Mollusk shells	27.303 ± 0.218	31.536 (31.159–31.913)	This study
B8	42° 01′15″	101° 33′22″	926	Mollusk shells	21.395 ± 0.187	25.58 (24.982–26.177)	This study
B9			923	Carbonate	20.83 +0.990/−0.840		Pachur et al. (1995)

1974). The land surface reflectance was determined by the underlying surface conditions. Reconstructions of paleovegetation using pollen have indicated that, during 34–26 cal kyr BP, coniferous forest could be found in the upper reaches (Herzschuh et al. 2006), steppe vegetation in the middle reaches (Zhang et al. 2002a), and desert steppe in the lower reaches. Therefore, the land surface reflectance values were set to 0.12, 0.17, and 0.20, respectively (Budyko & Miller 1974).

The surface emissivity (ε) is less affected by the underlying surface, and the average value is considered to be 0.95 for a land surface (Budyko & Miller 1974) and 0.96 for a water surface (Sellers 1965, Hastenrath & Kutzbach 1983, 1985). Therefore, an ε value of 0.95 was selected for the land surface in this study, and 0.96 was used for the water surface.

At the regional scale, the climate was warmer and wetter in western China, with an estimated annual temperature that was 2 to 4°C higher on the Tibet Plateau at that time than at present (Shi et al. 2001, Yu et al. 2007). A high tree pollen percentage for species such as *Picea*, *Betula* and *Juniperus* during 34–26 cal kyr BP has been discovered in the lake at an elevation of 3200 m, in the mountainous area of the upper reaches of the Heihe River. This indicates

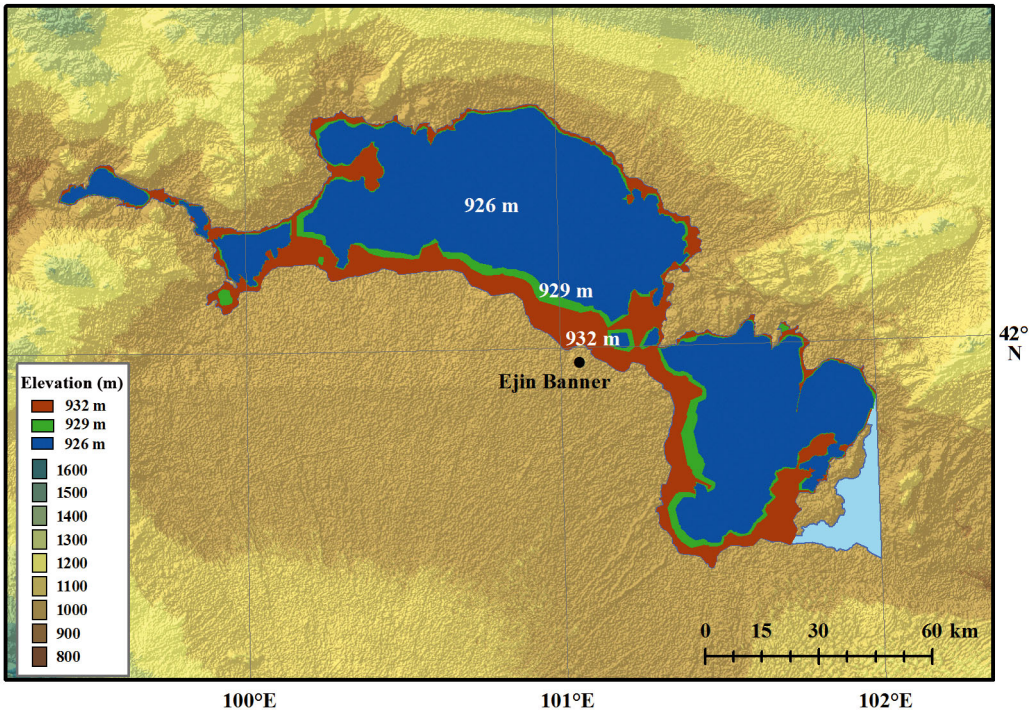

Fig. 3. Reconstruction results of the areas and extents of the Juyanze paleolake (altitude of 932 m a.s.l. at 34 cal kyr BP, 929 m a.s.l. at 32 cal kyr BP, and 926 m a.s.l. at 26 cal kyr BP). Light blue shade: possible lake area at 34 cal kyr BP

Table 4. Paleo-environmental parameters and evaporation calculated for the Heihe River catchment during 34–26 cal kyr BP. *E* (evaporation) was calculated using Eqs. (1) to (3)

Parameters	Unit	Upper reaches	Middle reaches	Lower reaches		References
				Land area	Water area	
34 cal kyr BP						
G	W m^{-2}	349.2	348	344.8	344.8	Berger (1978)
K		0.77	0.77	0.77	0.77	Xu (1994)
C		0.65	0.58	0.48	0.48	Jia et al. (2004)
α		0.12	0.17	0.20	0.08	Budyko & Miller (1974)
ε		0.95	0.95	0.95	0.96	Hastenrath & Kutzbach (1985)
T	K	273	282.5	284	286	Zhang et al. (2002a), Lu et al. (2007)
e	mb	4.2	4.4	7	9	Jia et al. (2004)
B		0.5	2	3	−0.579	Li et al. (2013)
A		0.19	0.21	0.20	0.27	This study
R′	W m^{-2}	25.97	21.37	40.36	28.68	This study
E	mm	225	92	131	885	This study
32 cal kyr BP						
G	W m^{-2}	349.8	348.7	345.5	345.5	Berger (1978)
K		0.77	0.77	0.77	0.77	Xu (1994)
C		0.62	0.61	0.53	0.53	Jia et al. (2004)
α		0.12	0.17	0.20	0.08	Budyko & Miller (1974)
ε		0.95	0.95	0.95	0.96	Hastenrath & Kutzbach (1985)
T	K	270	279.5	281	283	Zhang et al. (2002a), Lu et al. (2007)
e	mb	4.9	5.0	7	9	Jia et al. (2004)
B		0.5	2	3	−0.579	Li et al. (2013)
A		0.194	0.195	0.192	0.263	This study
R′	W m^{-2}	34.53	22.81	35.55	23.21	This study
E	mm	299	99	115	716	This study
26 cal kyr BP						
G	W m^{-2}	346.6	345.4	342.3	342.3	Berger (1978)
K		0.77	0.77	0.77	0.77	Xu (1994)
C		0.56	0.53	0.45	0.45	Jia et al. (2004)
α		0.12	0.17	0.20	0.08	Budyko & Miller (1974)
ε		0.95	0.95	0.95	0.96	Hastenrath & Kutzbach (1985)
T	K	274	283.5	285	287	Zhang et al. (2002a), Lu et al. (2007)
e	mb	6.3	4.5	5.8	7.8	Jia et al. (2004)
B		0.5	2	3	−0.579	Li et al. (2013)
A		0.193	0.217	0.216	0.292	This study
R′	W m^{-2}	44.74	28.24	39.21	25.16	This study
E	mm	387	122	127	776	This study

that the altitude of the forest line was 600 m higher than at present (Herzschuh et al. 2006). Thus, it can be inferred that the temperature was 3°C higher during 34–26 cal kyr BP. In the middle and lower reaches of the Heihe River, fossils of ostracods (*Limnocythere inopinata* and *Ilyocypris gibba*) have been discovered in the Duantouliang Profile of the Tengger Desert, indicating that the water temperature was 3°C higher than today (Zhang et al. 2002a). Quantitative reconstructions of the temperature have suggested that the temperature differences in western China between 34–26 cal kyr BP and the present are +2.1°C (34.1 cal kyr BP), −1.2°C (31.7 cal kyr BP), and +2.6°C (25.4 cal kyr BP) (Lu et al. 2007). Hence, in this study, the mean annual temperatures can be assumed to be 2°C higher in 34 cal kyr BP, 1°C lower in 32 cal kyr BP, and 3°C higher in 26 cal kyr BP than at the present. In addition, the lake surface temperature was 2°C higher than that of the land surface in the corresponding period (Yu et al. 2001). Based on data from the meteorological station, the modern mean annual temperatures from the upper to lower reaches are −2, 7.5, and 9°C, respectively. The relevant paleotemperature parameters are presented in Table 4.

The water surface Bowen ratio was set to −0.579, as has been demonstrated by Li et al. (2013). The land surface Bowen ratio (B_L) used in paleoclimate simulations is usually determined by the underlying surface (Yu et al. 2001). Here, the B_L values for the coniferous forest vegetation, steppe vegetation, and desert steppe were set to 0.5, 2, and 3, respectively (Yu et al. 2001).

The Ångström coefficient and R' were then calculated using Eqs. (3) and (2), respectively. All the paleo-environment parameters for 34–26 cal kyr BP are presented in Table 4.

4.3. Calculating evaporation

Using Eqs. (1) to (3) with the paleo-environmental parameters obtained from previous studies (Table 4), the water surface and land surface evaporation at the Juyanze paleolake were estimated to be 885 and 131 mm yr^{-1}, respectively, at around 34 cal kyr BP, and 776 and 127 mm yr^{-1}, respectively, at around 26 cal kyr BP (Table 4).

4.4. Reconstruction of catchment paleo-precipitation and paleo-runoff

Catchment paleo-precipitation during 34–26 cal kyr BP was calculated using Eqs. (1) to (4), and the results are presented in Table 5. The values of E_u, E_m, and E_l in Eq. (4) are shown in Table 4. The results revealed that the ratio between catchment paleo-precipitation and lake evaporation (P/E_w) during 34–26 cal kyr BP was approximately 3 times larger than that of the present, which indicates that the amount of effective precipitation during 34–26 cal kyr BP was much higher than that of the present.

Runoff from rivers to the lake during 34–26 cal kyr BP was calculated using Eqs. (1) to (3) and (5). In Eq. (5), we assumed $P_w \approx 70$ mm yr^{-1}. This was inferred from the anchored dune formation in the Badain Jaran Desert, which indicates that the precipitation amount was twice that of the present (Yang & Scuderi 2010). The results demonstrate that runoff from rivers to the lake during 34–26 cal kyr BP was higher than that of the present (Table 5).

Table 5. Reconstruction results for paleo-precipitation P, water surface evaporation E_w, and runoff R from rivers to the lake during 34–26 cal kyr BP

cal kyr BP	P (mm)	E_w (mm)	P/E_w	R (10^8 m^3)
34	177	885	0.2	61.95
32	164	716	0.23	38.85
26	189	776	0.24	39.46
0[a]	134	2345	0.06	9.26[b]

[a]From meteorological data
[b]Runoff in the lower reaches of the Heihe River, larger than runoff from rivers to the lake

5. DISCUSSION

5.1. Evaluation of the model

The water and energy balance equations have fewer parameters in a quantitative or semi-quantitative hydrologic budget model compared to other models. Therefore, this type of model has been applied to reconstructions of past hydrologic changes in drainage basins (Kutzbach 1980, Hastenrath & Kutzbach 1983, 1985, Bergonzini et al. 1997, Hoelzmann et al. 2000, Jia et al. 2001, Rhode et al. 2010, Huth et al. 2015). Nevertheless, there are some factors that could influence the reconstruction results, such as simplification of the model and uncertainty in the input variables (Li et al. 2013). Moreover, it is difficult to quantitatively estimate errors in the reconstruction (Jia et al. 2004). An approach that can be used to improve the accuracy and estimate the reliability of the reconstruction results is to calculate the present-day situation according to modern meteorological data and then correct the parameters (Li et al. 2013). Furthermore, model sensitivity and error estimates can provide realistic maximum magnitudes of error for each estimate (Bergonzini et al. 1997, Huth et al. 2015).

The model is calculated using annual mean values, and in areas with freezing wintertime temperatures, the water surface reflectivity ($\alpha = 0.08$) is likely to be low. However, the ratio of the evaporation in winter to the annual evaporation is only 5 to 7%, and the lake is iced over for less than 2 mo in winter. During 34–26 cal kyr BP, winter temperature was higher in most mid and lower latitudes of East Asia (Jiang et al. 2015), indicating that the duration of ice coverage was shorter than at present. Thus, calculating the annual evaporation using the annual mean values may have only a slight impact on the results. In our previous study (Li et al. 2013), we estimated the reliability of the reconstruction using modern meteorological data (annual mean values), and found that the difference between the observed and simulated annual evaporation values was −33 mm, with an error of 1.4% (Table 1). Moreover, the water and energy balance equations were calibrated using modern meteorological data in the lower reaches of the Heihe River, and as Table 1 shows, the equations have high accuracy.

Here, we rated variable sensitivity by the magnitude of the changes in P and R resulting from the likely error in an input variable. Realistic maximum error magnitudes for C and e were ±5%, which were calculated based on the work of Jia et al. (2000, 2001,

2004). Moreover, the results for the temperature reconstruction suggested that there were 1 to 2°C differences in the different proxy records (Thompson et al. 1997, Lu et al. 2007, Zheng et al. 2007). Therefore, we set the bounding error for temperature at ±2 K. The error estimates for the Bowen ratio for different underlying surfaces were considered to be ±5% (Yu et al. 2001).

Table 6 shows that the precipitation model is less sensitive to input parameters, with a 5% change giving a 5% change in *P*. However, the paleo-runoff model is sensitive to *C*, with a 5% change giving a more than 15% change in *R*. Moreover, uncertainties in the input variables also affect the results of P/E_w. To account for errors in the paleo-precipitation and paleo-runoff estimates due to the uncertainties in input variables, we calculated all the errors for each parameter estimate. Fig. 4 provides realistic maximum magnitudes of error for each parameter estimate, including the upper and lower bounding error. According to the errors calculated, we estimated that the catchment of the Heihe River required approximately 177 ± 29 mm yr^{-1} of precipitation to sustain the maximum lake area, a 32% increase over the modern value. We estimated runoff from rivers to the lake at 34 cal kyr BP to be 61.9 × 10^8 m^3, with an error of ±22.3 × 10^8 to 29.7 × 10^8 m^3. Moreover, we estimated catchment precipitation and runoff from rivers to the lake between 32 and 26 cal kyr BP to be 164 to 189 mm yr^{-1} and 38.9 × 10^8 to 39.5 × 10^8 m^3, respectively, with errors of ±26 to 30 mm yr^{-1} and ±14.3 × 10^8 to 15.9 × 10^8 m^3. This revealed that uncertainty in the input variables influenced the calculated results of *E*, *P*, P/E_w, and *R*; however, the lower evaporation, higher precipitation, and higher runoff that occurred at 34–26 cal kyr BP would not have been changed substantially.

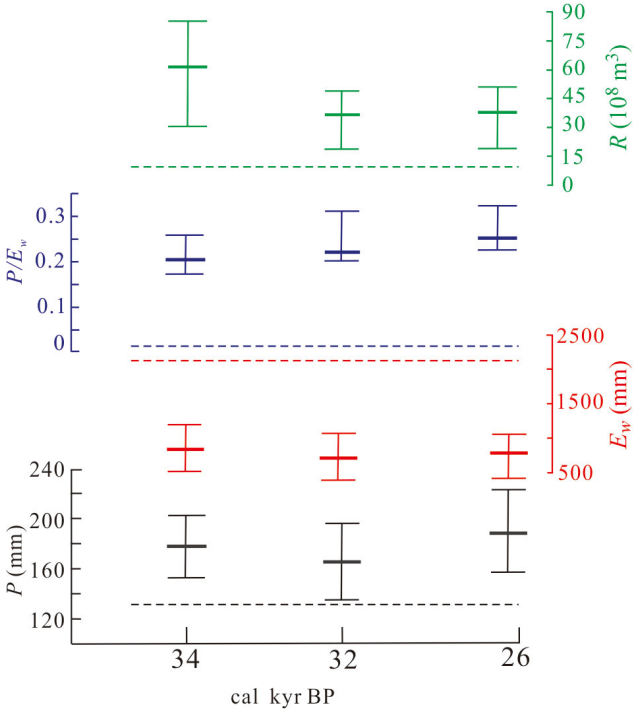

Fig. 4. Simulations of climate and hydrology conditions at highstand shorelines during the periods of 34, 32, and 26 cal kyr BP (thick horizontal bars). Error bars: reasonable maximum magnitudes of error for each parameter estimate. Dashed lines: averages for recent years (1961 to 2010)

5.2. Main factors influencing evolution of the Juyanze paleolake

The evolution of the lake was influenced by climatic and non-climatic factors. Previous studies have suggested that there were strong, young tectonic activities (induced subsidence) that had a large impact on the lake formations in the basin (Zhang et al. 2006, 2013, Hartmann & Wünnemann 2009). Hartmann (2003) suggested widespread features of faults

Table 6. Bounding error calculations for the highstand shoreline (34 cal kyr BP). Responses of model parameters (E_w, *P*, P/E_w, *R*) to a +5% (first value) or −5% (second value) change of an input parameter (*C*, *T*, *e*, *B*, *S*). Percent change of model parameter in parentheses

	Δ*C* (±5%)	Δ*T* (±2K)	Δ*e* (±5%)	Δ*B* (±5%)	Δ*S* (±5%)
E_w (mm)	735 (−17%), 1035 (+17%)	799 (−10%), 927 (+5%)	888 (+4%), 789 (−11%)	828 (−6%), 955 (+8%)	885 (0%), 885 (0%)
P (mm)	170 (−4%), 188 (+6%)	175 (−1%), 182 (+3%)	183 (+2%), 169 (−6%)	172 (−4%), 188 (+5%)	182 (+1.4%), 177 (−1.4%)
P/E_w	0.231 (+15.5%), 0.181 (−9%)	0.220 (+10%), 0.196 (−1.8%)	0.206 (+2%), 0.214 (+6%)	0.208 (+2%), 0.197 (−3%)	0.206 (+1%), 0.200 (−1%)
R (10^8 m^3)	50.5 (−18.5%), 73.3 (+18.3%)	55.4 (−10.6%), 65.1 (+5%)	62.18 (+4%), 54.65 (−12%)	57.62 (−7%), 67.27 (+9%)	65.05 (+5%), 58.85 (−5%)

within the entire basin, and Hölz et al. (2007) later confirmed the main lineaments. Dating of the lake deposits within and between geomorphological units also yielded a chronological framework of the tectonic movements and environmental changes, indicating an increasing subsidence rate since marine isotope stage (MIS) 4 within the whole basin. The subsidence is accompanied by the reactivation of the south–north-striking Gurinei graben structure forming the eastern boundary of the pull-apart basin (Becken et al. 2007). At the Juyanze paleolake, a strong subsidence in the northern part of the basin has been occurring since 18 cal kyr BP (Zhang et al. 2006, Hartmann et al. 2009). Since then, in terms of hydrology, the 3 terminal lakes that were once connected have become separated (Hartmann & Wünnemann 2009). This would explain the differences in sedimentation behavior between the Gaxun Nur and the Juyanze paleolake during the Holocene period. In addition, the elevations of the lake levels would have decreased accordingly. In this case, the altitudes of the paleoshorelines would have been influenced by the subsidence, and the actual altitudes of the lake levels during 34–26 cal kyr BP might have been higher than our measurements. In other words, the Juyanze paleolake areas and our calculated catchment paleo-precipitation and runoff from rivers to the lake values at 34 cal kyr BP might be underestimated. However, the reasons for the lake level fluctuations during 34–26 cal kyr BP are still uncertain, but 2 explanations might be applied. (1) Tectonic activities (subsidence) caused the lake levels to decrease; (2) changes in precipitation and other climatic factors drove the fluctuations. Fig. 4 indicates that there were slight changes in P and P/E_w between 32 and 26 cal kyr BP; however, the changes may have been caused by errors in calculation. Hence, the mechanism by which the lake levels fluctuated during 34–26 cal kyr BP remains uncertain. In summary, tectonic activities could not have produced the high lake levels of the Juyanze paleolake during 34–26 cal kyr BP, but lake level fluctuations on a millennial timescale during 34–26 cal kyr BP might have been affected by tectonic activities or other factors.

Climatic change, as another important factor, also influences lake evolution. In arid regions, water-level changes of inland lakes are a result of the balance between precipitation, runoff, and evaporation (Li & Morrill 2010). Hence, the fluctuation of lake levels was influenced by climatic factors including catchment precipitation, runoff, and evaporation, and changes in these factors could have caused the lake levels to fluctuate (Li & Morrill 2010). Higher catchment precipitation and river runoff often raise the water levels of lakes in an arid region, and vice versa (Li et al. 2013). In addition, lower evaporation also raises the water levels of lakes (Li & Morrill 2010). In this study, the catchment paleo-precipitation reconstruction results (Table 5, Fig. 4) suggest that higher catchment precipitation occurred during 34–26 cal kyr BP. Higher catchment precipitation can enhance the amount of runoff in an arid region, and the reconstruction results for runoff from rivers to the lake also suggest that this value was higher during 34–26 cal kyr BP than that at present (Fig. 4). Moreover, the P/E ratio can be interpreted as a proxy index for effective precipitation. A high ratio of P/E reflects high effective precipitation, and vice versa (Zhang et al. 2002b). Fig. 4 shows that a high P/E_w ratio occurred at 34–26 cal kyr BP, which indicates that the effective precipitation was higher than that at present. Therefore, a humid climate including high precipitation and low evaporation during 34–26 cal kyr BP was favorable for the formation of high lake levels in the Juyanze paleolake.

5.3. Regional significance

Our reconstructions of changes in lake level and paleoclimate for the Juyanze paleolake indicate that a humid climate including high precipitation and low evaporation occurred during 34–26 cal kyr BP. The Juyanze paleolake was controlled by the Indian monsoon and westerly winds (Mischke et al. 2003, Yang et al. 2011). However, because the Ejina Basin serves as a base for the Heihe River drainage system from the NE Tibetan Plateau, the upstream paleo-precipitation was also affected by the Indian monsoon (Li et al. 2012a). Therefore, the record of the climate signal is complex. To clarify whether our results reflect a local signal or regional record, we compared them with other proxy records for the NW Asian monsoon margin, the monsoon area of the southern Tibet Plateau, and the area influenced by westerly winds.

In the NW Asian monsoon margin, many proxy records suggest that a humid environment and high lake levels occurred during 40–25 cal kyr BP on the Alashan Plateau, such as in the Badain Jaran Desert (Yang et al. 2011) and the Tengger Desert (Pachur et al. 1995, Zhang et al. 2004, Wang et al. 2011). In the Badain Jaran Desert, along the southeastern side of the Juyanze paleolake, calcareous root tubes that were formed by pedogenic processes and that are indicative of increased effective moisture level were

distributed widely during 38–25 cal kyr BP, suggesting a humid environment (Yang et al. 2003, Li et al. 2015a,b). The Tengger Desert was characterized by large wetland areas during 34–26 cal kyr BP, and the high lake levels, supported by evidence of chemical deposition and pollen assemblages, suggest a humid environment (Zhang et al. 2002b). Therefore, most of the proxy records for this area reveal changes in the effective moisture and indicate that the climate during 34–26 cal kyr BP was humid (Zhang et al. 2002b, Yang et al. 2004, Yang & Scuderi 2010, Wang et al. 2011, Yang et al. 2011, Li et al. 2015a).

In the area influenced by westerly winds, many proxy records also suggest a humid environment during the previous period. Lacustrine deposits found over an area ranging from China's western Taklimakan Desert to the eastern Hunshandake Sandy Lands suggest that extensive lakes occurred in China's deserts at approximately 30 ka (Yang et al. 2011). Fluvial terraces along the Keriya River in the Taklimakan Desert suggest a wetter environment during 33 cal kyr BP (Yang et al. 2002). Moreover, optically stimulated luminescence (OSL) dating results have shown that 3 layers of lacustrine sediments formed between 40 and 30 ka in the interior of the Taklimakan Desert, also suggesting that parts of the desert were humid environments during roughly 40–30 ka (Yang et al. 2006). In addition, loess paleosol records from the Ili Basin of western Xinjiang have revealed poorly developed paleosols at 26.1 ka, which were dated by OSL (Ye et al. 2000). Thus, it can be inferred that there was a relatively warm and humid period during 34–26 cal kyr BP.

Humid environment and high lake levels occurred during 40–30 cal kyr BP in the Tibetan Plateau (Shi et al. 1999, Li 2000, Zhang et al. 2009, Kong et al. 2011). Li (2000) showed that paleolake areas expanded by 450% during this period, which was thus named the 'Greatest Lake Period'. Based on water budget modeling, Shi et al. (1999) suggested that the precipitation increased by 40 to 100%. Moreover, the Qarhan paleolake, located in the central Qaidam Basin, was fully developed, with its maximum level occurring during approximately 37.8–31.9 cal kyr BP, indicating a warm-humid climate (Zhang et al. 2009). ^{10}Be and ^{26}Al dating of the paleolake shorelines in the Tibetan Plateau has also suggested that high lake levels occurred in a similar period (Kong et al. 2011).

It appears that it was more humid both in the deserts because of the influence of the Asian summer monsoon, and in the areas where moisture is currently associated with westerlies. In addition, a humid climate was also revealed in the Tibetan Plateau areas. Although it could not be further confirmed with other proxy records that high precipitation and/or low evaporation resulted in a humid environment in the area influenced by westerly winds, this does suggest that high effective precipitation occurred during 34–26 cal kyr BP. Thus, the high lake levels and humid climate of the Juyanze paleolake were not a local signal but a regional record.

Possible causes for the humid climate in this region during 34–26 cal kyr BP have been proposed by Yu et al. (2005, 2007). Based upon paleoclimate modeling, Yu et al. (2007) suggested that Quaternary ice sheets in the Northern Hemisphere played an important role in temperature decreases at mid-high latitudes, and also enhanced the south–north temperature gradients. These, in turn, increased moisture transport from low to high latitudes and increased monsoonal precipitation over the Tibetan Plateau. Moreover, vegetation changes in East Asia occurred as a result of increased temperature in the low latitudes, an extended rain-belt reaching northwards into China, and an enlarged area of increased precipitation inland (Yu et al. 2005, 2007).

6. CONCLUSIONS

Fourteen paleoshorelines were recognized at the Juyanze paleolake, and ^{14}C showed that the highest 8 formed during 34–26 cal kyr BP. Therefore, the Juyanze paleolake had high lake levels during 34–26 cal kyr BP, and these fluctuated at different timescales. A unified Juyanze paleolake with an area of 7601 km^2 and an altitude of 932 m a.s.l. occurred at 34 cal kyr BP. It then decreased to 6104 km^2 with an altitude of 930 m a.s.l. at 32 cal kyr BP and to 5589 km^2 with an altitude of 926 m a.s.l. at 26 cal kyr BP. Tectonic activities could not have produced the high lake levels during 34–26 cal kyr BP; however, tectonic activities or other factors may have affected the lake level fluctuations at the millennial timescale during this period.

Catchment paleo-precipitation and paleo-runoff reconstructions showed that the catchment of the Heihe River required approximately 177 ± 29 mm yr^{-1} of precipitation to sustain the maximum lake area, which is a 32% increase compared with the modern value. Water evaporation was only 30% of present values. Runoff from rivers to the lake was 61.9×10^8 m^3 at 34 cal kyr BP, with an error of $\pm 22.3 \times 10^8$ to 29.7×10^8 m^3. We also estimated catchment precipitation and runoff from rivers to the lake,

which were 164 to 189 mm yr^{-1} and 38.9 × 10^8 to 39.5 × 10^8 m^3 between 32 and 26 cal kyr BP, with errors of ±26 to −30 mm yr^{-1} and ±14.3 × 10^8 to 15.9 × 10^8 m^3, respectively. Uncertainty in the input variables influenced the calculated results of E, P, P/E_w, and R. However, these errors would not have affected the results of lower evaporation, higher precipitation, and higher runoff at MIS 3a substantially. Therefore, a humid climate including high precipitation and low evaporation occurred during 34–26 cal kyr BP and this was favorable for the formation of high lake levels at the Juyanze paleolake.

The humid climate and high lake levels of the Juyanze paleolake that occurred during 34–26 cal kyr BP were a regional record. They may have been produced by the significantly increased precipitation, which was directly related to an enhanced monsoon resulting from increased temperature contrasts between higher and lower latitudes under larger latitudinal gradients of insolation and stronger ice sheet impacts at 34–26 cal kyr BP than at present. Moreover, low levels of evaporation may also have affected moisture changes, but it remains uncertain whether this is a local signal or a regional record.

Acknowledgements. We thank 2 anonymous reviewers for their constructive comments, which led to significant improvement of the manuscript. The study was supported by the National Natural Science Foundation of China (Nos. 41530745 and 41301217) and the Fundamental Research Funds for the Central Universities (lzujbky-2015-148).

LITERATURE CITED

Becken M, Hölz S, Fiedler-Volmer R, Hartmann K, Wünnemann B, Burkhardt H (2007) Electrical resistivity image of the Jingsutu Graben at the NE margin of the Ejina Basin (NW China) and implications for the basin development. Geophys Res Lett 34:L09315, doi:10.1029/2007GL029412

Berger A (1978) Long-term variations of daily insolation and Quaternary climatic changes. J Atmos Sci 35:2362–2367

Bergonzini L, Chalié F, Gasse F (1997) Paleoevaporation and paleoprecipitation in the Tanganyika basin at 18,000 years BP inferred from hydrologic and vegetation proxies. Quat Res 47:295–305

Berliand ME, Berliand TG (1952) Determining the net longwave radiation of the Earth with consideration of the effect of cloudiness. Izv Akad Nauk SSSR Ser Geofiz 1: 64–78 (in Russian)

Budyko MI, Miller DH (1974) Climate and life, Vol 508. Academic press, New York, NY

Conroy JL, Overpeck JT (2011) Regionalization of present-day precipitation in the greater monsoon region of Asia. J Clim 24:4073–4095

Ding R, Wang F, Wang J, Liang J (2009) Analysis on spatial-temporal characteristics of precipitation in Heihe River Basin and forecast evaluation in recent 47 years. J Desert Res 29:335–341 (in Chinese with English abstract)

Gracia Prieto F (1995) Shoreline forms and deposits in Gallocanta Lake (NE Spain). Geomorphology 11:323–335

Hartmann K (2003) Spätpleistozäne und holozäne Morphodynamik im nördlichen Gaxun Nur Becken, Innere Mongolei, NW China. PhD thesis, Freie Universität Berlin

Hartmann K, Wünnemann B (2009) Hydrological changes and Holocene climate variations in NW China, inferred from lake sediments of Juyanze palaeolake by factor analyses. Quat Int 194:28–44

Hartmann K, Wünnemann B, Zhang H (2009) Neotectonic impact and Palaeohydrology of Gaxun Nur Basin (NW China) during the Late Quaternary. Geophys Res Abstr 11:EGU2009-6330, http://meetingorganizer.copernicus.org/EGU2009/EGU2009-6330.pdf

Hastenrath S, Kutzbach JE (1983) Paleoclimatic estimates from water and energy budgets of East African lakes. Quat Res 19:141–153

Hastenrath S, Kutzbach J (1985) Late Pleistocene climate and water budget of the South American Altiplano. Quat Res 24:249–256

Herzschuh U, Kürschner H, Mischke S (2006) Temperature variability and vertical vegetation belt shifts during the last ~50,000 yr in the Qilian Mountains (NE margin of the Tibetan Plateau, China). Quat Res 66:133–146

Hoelzmann P, Kruse HJ, Rottinger F (2000) Precipitation estimates for the eastern Saharan palaeomonsoon based on a water balance model of the West Nubian Palaeolake Basin. Global Planet Change 26:105–120

Hölz S, Polag D, Becken M, Fiedler-Volmer R, Zhang HC, Hartmann K, Burkhardt H (2007) Electromagnetic and geoelectric investigation of the Gurinai Structure, Inner Mongolia, NW China. Tectonophysics 445:26–48

Huth T, Hudson AM, Quade J, Guoliang L, Hucai Z (2015) Constraints on paleoclimate from 11.5 to 5.0 ka from shoreline dating and hydrologic budget modeling of Baqan Tso, southwestern Tibetan Plateau. Quat Res 83: 80–93

Jia Y, Shi Y, Fan Y (2000) Water balance of paleolake Qinghai and its precipitation estimation at three high lake-level stages since 40 ka BP. J Lake Sci 12:211–218 (in Chinese with English abstract)

Jia Y, Shi Y, Cao J, Fan Y (2001) The precipitation of the interior lakes in the southwestern Tibetan Plateau at 40–30 ka BP. Adv Earth Sci 16:346–351 (in Chinese with English abstract)

Jia Y, Ma C, Zhu C, Wei L, Wang P (2004) Past, present and future of estimates of paleoprecipitation in closed lake basin. Sci Geogr Sin 24:376–383 (in Chinese with English abstract)

Jiang H, Mao X, Xu H, Thompson J, Wang P, Ma X (2011) Last glacial pollen record from Lanzhou (northwestern China) and possible forcing mechanisms for the MIS 3 climate change in Middle to East Asia. Quat Sci Rev 30: 769–781

Jiang D, Yu G, Zhao P, Chen X and others (2015) Paleoclimate modeling in China: a review. Adv Atmos Sci 32: 250–275

Kong P, Na C, Brown R, Fabel D, Freeman S, Xiao W, Wang Y (2011) Cosmogenic ^{10}Be and ^{26}Al dating of paleolake shorelines in Tibet. J Asian Earth Sci 41:263–273

Kutzbach JE (1980) Estimates of past climate at Paleolake Chad, North Africa, based on a hydrological and energy-balance model. Quat Res 14:210–223

Lazarus ED, Murray AB (2011) An integrated hypothesis for

regional patterns of shoreline change along the Northern North Carolina Outer Banks, USA. Mar Geol 281:85–90

Lehmkuhl F, Haselein F (2000) Quaternary paleoenvironmental change on the Tibetan Plateau and adjacent areas (Western China and Western Mongolia). Quat Int 65–66:121–145

Li B (2000) The last greatest lakes on the Xizang (Tibetan) Plateau. Acta Geol Sin 55:174–182 (in Chinese with English abstract)

Li Y, Morrill C (2010) Multiple factors causing Holocene lake-level change in monsoonal and arid central Asia as identified by model experiments. Clim Dyn 35: 1119–1132

Li Y, Wang N, Chen H, Li Z, Zhou X, Zhang C (2012a) Tracking millennial-scale climate change by analysis of the modern summer precipitation in the marginal regions of the Asian monsoon. J Asian Earth Sci 58:78–87

Li Y, Wang NA, Li ZL, Zhang CQ, Zhou XH (2012b) Reworking effects in the Holocene Zhuye Lake sediments: a case study by pollen concentrates AMS ^{14}C dating. Sci China Earth Sci 55:1669–1678

Li Z, Wang N, Li Y, Zhang Z, Li M, Dong C, Huang R (2013) Runoff simulations using water and energy balance equations in the lower reaches of the Heihe River, northwest China. Environ Earth Sci 70:1–12

Li Z, Wang N, Cheng H, Ning K, Zhao L, Li R (2015a) Formation and environmental significance of Late Quaternary calcareous root tubes in the deserts of the Alashan Plateau, northwest China. Quat Int 372:167–174

Li Z, Wang N, Li R, Ning K, Cheng H, Zhao L (2015b) Indication of millennial-scale moisture changes by the temporal distribution of Holocene calcareous root tubes in the deserts of the Alashan Plateau, northwest China. Palaeogeogr Palaeoclimatol Palaeoecol 440:496–505

Long H, Lai Z, Fuchs M, Zhang J, Li Y (2012) Timing of Late Quaternary palaeolake evolution in Tengger Desert of northern China and its possible forcing mechanisms. Global Planet Change 92-93:119–129

Lu H, Wu N, Liu K, Jiang H, Liu T (2007) Phytoliths as quantitative indicators for the reconstruction of past environmental conditions in China. II. Palaeoenvironmental reconstruction in the Loess Plateau. Quat Sci Rev 26: 759–772

Ma N, Wang N, Li Z, Chen X, Zhu J, Dong C (2011) Analysis on climate change in the northern and southern marginal zones of the Badain Jaran Desert during the period 1960–2009. Arid Zone Res 28:242–250 (in Chinese with English abstract)

Mischke S, Demske D, Schudack M (2003) Hydrologic and climatic implications of a multidisciplinary study of the Mid to Late Holocene Lake Eastern Juyanze. Chin Sci Bull 48:1411–1417

Pachur HJ, Wünnemann B, Zhang H (1995) Lake evolution in the Tengger Desert, northwestern China, during the last 40,000 years. Quat Res 44:171–180

Pigati JS, Rech JA, Nekola JC (2010) Radiocarbon dating of small terrestrial gastropod shells in North America. Quat Geochronol 5:519–532

Reimer PJ, Bard E, Bayliss A, Beck JW and others (2013) IntCal13 and MARINE13 radiocarbon age calibration curves 0–50 000 years cal BP. Radiocarbon 55:1869–1887

Rex R (1961) Hydrodynamic analysis of circulation and orientation of lakes in northern Alaska. In: Raasch GO (ed) Geology of the Arctic, Vol 2. University of Toronto Press, Toronto, p 1021–1043

Rhode D, Haizhou M, Madsen DB, Brantingham PJ, Forman SL, Olsen JW (2010) Paleoenvironmental and archaeological investigations at Qinghai Lake, western China: geomorphic and chronometric evidence of lake level history. Quat Int 218:29–44

Sellers WD (1965) Physical climatology, Vol 111. University of Chicago Press, Chicago, IL

Shen Y, Li S, Chen Y, Qi Y, Zhang S (2013) Estimation of regional irrigation water requirement and water supply risk in the arid region of northwestern China 1989–2010. Agric Water Manage 128:55–64

Shi Y, Liu X, Li B (1999) The very strong summer monsoon event of 40–30 ka BP in Qinghai-Xizang Plateau and its relationship to the precession period. Chin Sci Bull 44: 1475–1480 (in Chinese)

Shi Y, Yu G, Liu X, Li B, Yao T (2001) Reconstruction of the 30–40 ka BP enhanced Indian monsoon climate based on geological records from the Tibetan Plateau. Palaeogeogr Palaeoclimatol Palaeoecol 169:69–83

Thompson L, Yao T, Davis M, Henderson K and others (1997) Tropical climate instability: the last glacial cycle from a Qinghai-Tibetan ice core. Science 276:1821–1825

Wang N, Li Z, Cheng H, Li Y, Huang Y (2011) High lake levels on Alxa Plateau during the Late Quaternary. Chin Sci Bull 56:1799–1808

Xu Z (1994) Meteorology. China Meteorological Press, Beijing

Yan L, Zheng M (2015) The response of lake variations to climate change in the past forty years: a case study of the northeastern Tibetan Plateau and adjacent areas, China. Quat Int 371:31–48

Yang X, Scuderi LA (2010) Hydrological and climatic changes in deserts of China since the late Pleistocene. Quat Res 73:1–9

Yang X, Zhu ZD, Jaekel D, Owen LA, Han JM (2002) Late Quaternary palaeoenvironment change and landscape evolution along the Keriya River, Xinjiang, China: the relationship between high mountain glaciation and landscape evolution in foreland desert regions. Quat Int 97-98:155–166

Yang X, Liu T, Xiao H (2003) Evolution of megadunes and lakes in the Badain Jaran Desert, Inner Mongolia, China during the last 31,000 years. Quat Int 104:99–112

Yang B, Shi Y, Braeuning A, Wang J (2004) Evidence for a warm-humid climate in arid northwestern China during 40–30 ka BP. Quat Sci Rev 23:2537–2548

Yang XP, Preusser F, Radtke U (2006) Late Quaternary environmental changes in the Taklamakan Desert, western China, inferred from OSL-dated lacustrine and aeolian deposits. Quat Sci Rev 25:923–932

Yang X, Scuderi L, Paillou P, Liu Z, Li H, Ren X (2011) Quaternary environmental changes in the drylands of China — a critical review. Quat Sci Rev 30:3219–3233

Ye W, Dong GR, Yuan YJ, Ma YJ (2000) Climate instability in the Yili region, Xinjiang during the last glaciation. Chin Sci Bull 45:1604–1609

Yu G, Shen H (2010) Lake water changes in response to climate change in northern China: simulations and uncertainty analysis. Quat Int 212:44–56

Yu G, Xue B, Liu J, Chen X, Zheng Y (2001) Lake records from China and the palaeoclimate dynamics. China Meteorological Press, Beijing

Yu G, Zheng Y, Ke X (2005) 35 ka BP climate simulations in East Asia and probing the mechanisms of climate changes. Chin Sci Bull 50:58–67

Yu G, Gui F, Shi Y, Zheng Y (2007) Late marine isotope stage 3 palaeoclimate for East Asia: a data–model comparison. Palaeogeogr Palaeoclimatol Palaeoecol 250:167–183

Zhang HC, Ma YZ, Peng JL, Li JJ and others (2002a) Palaeolake and palaeoenvironment between 42 and 18 ka BP in Tengger Desert, NW China. Chin Sci Bull 47: 1946–1956

Zhang HC, Wunnemann B, Ma YZ, Peng JL and others (2002b) Lake level and climate changes between 42,000 and 18,000 ^{14}C yr BP in the Tengger Desert, northwestern China. Quat Res 58:62–72

Zhang HC, Peng JL, Ma YZ, Chen GJ and others (2004) Late Quaternary palaeolake levels in Tengger Desert, NW China. Palaeogeogr Palaeoclimatol Palaeoecol 211: 45–58

Zhang HC, Ming QZ, Lei GL, Zhang WX and others (2006) Dilemma of dating on lacustrine deposits in an hyperarid inland basin of NW China. Radiocarbon 48:219–226

Zhang HC, Zhang WX, Chang FQ, Yang LQ and others (2009) Geochemical fractionation of rare earth elements in lacustrine deposits from Qaidam Basin. Sci China Ser D: Earth Sci 52:1703–1713

Zhang HC, Chang FQ, Chen GJ, Zhen Q, Cai YF, Li H (2013) Human impact on climate and eco-hydrological systems in the Badain Jaran desert in northwest China. E3 J Environ Res Manage 4:310–317

Zhao Y, Yu Z, Chen F, Ito E, Zhao C (2007) Holocene vegetation and climate history at Hurleg Lake in the Qaidam Basin, northwest China. Rev Palaeobot Palynol 145: 275–288

Zheng MP, Yuan HR, Liu JY, Li YH, Ma ZB, Sun Q (2007) Sedimentary characteristics and paleoenvironmental records of Zabuye Salt Lake, Tibetan Plateau, since 128 ka BP. Acta Geol Sin 81:861–879

Editorial responsibility: Balaji Rajagopalan, Boulder, Colorado, USA

Submitted: September 7, 2015; Accepted: May 20, 2016
Proofs received from author(s): June 30, 2016